Optimal Power Control for Underlay Cognitive Radio Systems With Arbitrary Input Distributions

Gozde Ozcan and M. Cenk Gursoy

***Abstract*—This paper studies optimal power control policies that maximize the achievable rates of underlay cognitive radio systems with arbitrary input distributions under both peak/average transmit power and peak/average interference power constraints for general fading distributions. In particular, optimal power adaptation schemes are formulated and low-complexity optimal power control algorithms are proposed. Additionally, simpler approximations of optimal power control policies in the low-power regime are determined. By considering gamma distributed channel power gains of the interference link between the secondary transmitter and the primary receiver and of the transmission link between the secondary transmitter and the secondary receiver, closed-form expressions for the maximum achievable rate attained with optimal power control in the low-power regime are provided. Through numerical results, the impact of the fading severity of both interference and transmission links and transmit power and interference power constraints on the maximum achievable rate of the cognitive user for different practical constellations and Gaussian signals are investigated.**

***Index Terms*—Cognitive radio, fading channels, interference power constraint, low-power regime, mutual information, MMSE, optimal power control, spectrum sharing, transmit power constraint, underlay cognitive radio.**

I. Introduction

IN THE SPAN of a decade, there have been rapid developments in the wireless technology, resulting in the proliferation of wireless devices, including smart phones, tablets, and handheld computers. It has been predicted that the number of wireless devices will reach around 100 billion by 2025 [1]. This explosive growth in wireless devices and new wireless applications prompts unprecedented demand on the radio spectrum. However, the radio spectrum is a finite natural resource and the prime portion of the RF spectrum (e.g., between 30 MHz to 3 GHz) has already been allocated to specific applications or services.

On the other hand, the Spectrum-Policy Task Force of the Federal Communications Commission (FCC) [2] reported that the spectrum scarcity problem is mainly due to the underutilization and inefficient usage in many portions of the spectrum rather than the limited range of usable frequencies. In light of this fact, cognitive radio has been proposed as an innovative technology to overcome the spectrum underutilization problem by allowing the unlicensed users (i.e., cognitive or secondary users) to access the licensed spectrum without causing harmful interference to the licensed users (i.e., primary users). Hence, this technology provides bright prospects for implementing flexible spectrum allocation strategies and opening up bandwidth for new wireless services. Since its first introduction by Mitola in 1999 [3], there has been intensive research on the performance of cognitive radios. As a result, the cognitive radio technology has become more mature for commercial use over the years. In this regard, standardization activities, such as by IEEE 802.22 [4] for unlicensed access in VHF/UHF TV broadcast bands between 54 MHz and 790 MHz, IEEE 802.11af (also referred to as White-Fi) [5] for WiFi technology over unused TV bands and IEEE SCC41 [6], and regulations such as by the FCC [7] in the US and other regulatory bodies in different countries, facilitate widespread operational adoption of this promising technology. Beyond TV white spaces, cognitive radio systems find applications to improve the spectrum utilization in cellular systems, wireless LANs, machine-to-machine communications, vehicle-to-vehicle networks, wireless e-health services, and public safety services [8], [9].

A. Literature Overview

One of the proposed communication models for cognitive radio is underlay transmission scheme [10]. Specifically, the underlay scheme enables transmission of cognitive users only if the interference at the primary receivers is kept below a certain threshold. To enhance the performance of underlay cognitive radio systems while providing sufficient protection for the licensed primary users, power adaptation strategies for different types of secondary users' data traffic have been extensively studied.

For delay-insensitive secondary user's data traffic such as email and file transfer, proper performance measure is the ergodic capacity, which characterizes the maximum achievable long-term data rate averaged over the channel fading states. In this regard, the authors in [11] considered power allocation policies for truncated channel inversion with fixed rate (TIFR) and truncated optimum rate allocation (ORA) transmission schemes to maximize the ergodic capacity of the secondary user subject to average or peak transmit power constraints together with interference power constraints in such a way that the minimum rate requirement for the primary receiver is satisfied

Manuscript received August 5, 2014; revised January 5, 2015; accepted March 8, 2015. Date of publication March 31, 2015; date of current version August 10, 2015. The material in this paper was presented in part at the IEEE Conference on Global Communications (Globecom), Austin, TX, USA, December 2014. The associate editor coordinating the review of this paper and approving it for publication was D. C. Popescu.

The authors are with the Department of Electrical Engineering and Computer Science, Syracuse University, Syracuse, NY 13244 USA (e-mail: gozcan@syr.edu; mcgursoy@syr.edu).

Color versions of one or more of the figures in this paper are available online at http://ieeexplore.ieee.org.

Digital Object Identifier 10.1109/TWC.2015.2418208

with a certain probability. In the TIFR scheme, the secondary transmitter adapts its power to keep the transmission rate constant at the secondary receiver by inverting the channel power gain while in truncated ORA scheme, the secondary transmitter uses the same transmit power for fading states above a certain cutoff fade depth. The authors in [12] obtained optimal power allocation strategies that maximize the ergodic capacity of the secondary user under either peak or average transmit power constraints together with a constraint on the outage capacity of the primary user, which requires the channel side information of the link between the primary transmitter and primary receiver to be known. In addition, the work in [13] mainly focused on the optimal power control strategies that maximize the ergodic capacity of the secondary user subject to peak/average transmit power constraints together with an upper bound on the outage capacity loss of the primary user due to secondary user transmission. In [14], optimal power allocation schemes that maximize the achievable rates of an OFDM-based cognitive radio system were determined.

If secondary users' data traffic is delay-sensitive such as in mobile streaming/interactive video and VoIP, a more suitable performance metric is the outage capacity, which quantifies the maximum achievable rate at a certain outage probability. Accordingly, in addition to ergodic capacity, the work in [15] considered the TIFR scheme to maximize the outage capacity of the secondary user subject to both peak and average interference power constraints. Also, the authors in [16] obtained the optimal power allocation strategies for the ergodic capacity, delay-limited capacity and the outage capacity of cognitive radio channels subject to peak/average transmit and peak/average interference constraints. Recently, the notion of effective capacity has been introduced for identifying the maximum throughput under statistical quality of service (QoS) constraints in the form of the limitations on the buffer overflow probability or delay-violation probability. In this respect, the authors in [17] conducted an analysis of the effective capacity in cognitive radio systems and studied the optimal power adaptation methods under average interference power constraints.

Sharing essentially the key demands of cognitive radios for improving spectrum utilization, throughput and energy consumption, device-to-device (D2D) communication has also been proposed in cellular networks as a new paradigm which allows direct communication between nearby devices coordinated by the central authority. Indeed, D2D communication can be conceptually considered as an extension of cognitive radio models in which the traditional cellular links can be regarded as primary transmission links and D2D links as secondary transmission links. In addition, both cognitive radios and D2D aim at utilizing the radio resources efficiently and successfully performing interference management. In this regard, the authors in [18] jointly determined the power allocation and mode selection schemes (e.g., whether to transmit via the direct D2D link (D2D mode) or the cellular base station (cellular mode)) to maximize the ratio of the system capacity to total power, called as the power-efficiency. The work in [19] mainly focused on the optimization of mode selection, system bandwidth and power allocation for D2D communications to minimize the overall transmission power. Also, the authors in [20] studied the problem of power control and mode selection for D2D communications in a cognitive cellular network. Moreover, the authors in [21] studied the statistical properties of the transmit power and signal to interference plus noise ratio (SINR) for D2D communication employing power control.

B. Main Contributions

In all of the aforementioned studies, the implicit assumption was that the input signal follows a Gaussian distribution, leading to elegant closed-form expressions for the optimal power allocation schemes. However, it may not be easy to realize Gaussian inputs in practice, and correspondingly inputs chosen from discrete constellations such as pulse amplitude modulation (PAM), quadrature amplitude modulation (QAM) and phase shift keying (PSK) are frequently employed in practical applications. Therefore, if the actual signal input distribution is not taken into account, considerable performance degradation may often occur for systems optimized under the Gaussian input assumption. This consideration motivates the research for more general power allocation schemes for underlay cognitive radio systems in which the input is not necessarily Gaussian distributed. Therefore, in this paper, we identify the optimal power control policies that maximize the achievable rates of secondary users with arbitrary input signaling. The main contributions of this paper can be summarized as follows:

- Exploiting the key relation between the mutual information and minimum mean square error (MMSE) [23], we obtain optimal power adaptation schemes to maximize the achievable rates of secondary users with arbitrary input signaling in underlay cognitive radio systems subject to peak/average transmit power constraints along with peak/average interference power constraints. Our results are different from the works in [22] and [24], where only average transmit power constraint is imposed to obtain optimal power control policy in a non-cognitive context. More specifically, beside the transmit power constraint at the secondary transmitter, we impose constraints on either peak or average received power at the primary receiver. Hence, the power has been adapted instantaneously according to the channel power gains of both the transmission link between the secondary transmitter and the secondary receiver and the interference link between the secondary transmitter and the primary receiver.
- Low-complexity optimal power control algorithms under peak/average transmit power and peak/average interference power constraints are proposed. The proposed algorithms do not impose any restrictions on the input distribution. Therefore, the proposed algorithms are applicable to more realistic and practical settings and are not restricted to the Gaussian input.
- We also conduct a low signal-to-noise ratio (SNR) (or equivalently low-power) analysis. The recent study in [25] obtained closed-form first-order ergodic capacity expressions for underlay cognitive radio systems operating in the low-SNR regime with Gaussian inputs and constraints on either the transmit power or interference power. Different

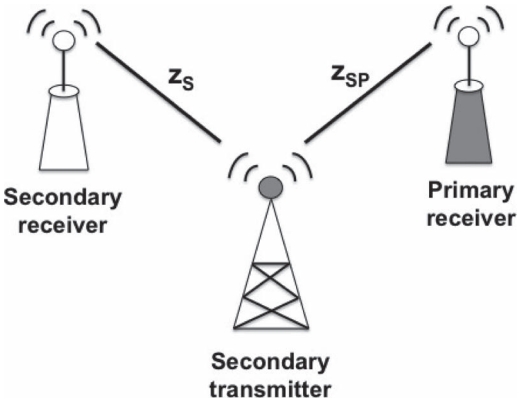

Fig. 1. Underlay cognitive radio system model.

from this work, we first analyze the optimal power control policies in the low-power regime for arbitrary input distributions subject to peak/average transmit power and peak/average interference power constraints and then derive closed-form second-order achievable rate expressions attained with the resulting optimal power expressions under peak transmit and interference power constraints and average transmit power constraint. In the latter analysis, the Nakagami-m fading model is used due to its flexibility in representing a wider range of fading severities [26].

The rest of the paper is organized as follows: Section II introduces the system model. In Section III, optimal power control policies that maximize the achievable rate of the secondary user with arbitrary input distributions subject to different combinations of transmit power and interference power constraints are determined and the optimal power control algorithms are provided. Subsequently, the low-power analysis is conducted in Section IV, where approximations to the optimal power control policies and the corresponding closed-form second-order achievable rate expressions are obtained. Numerical results are presented and discussed in Section V. Finally, main conclusions are drawn in Section VI. Proofs are relegated to the Appendix.

II. System Model

We consider an underlay cognitive radio system in which the secondary users coexist with the licensed primary users while satisfying certain interference constraints. The instantaneous *channel power gains* of the transmission link between the secondary transmitter and the secondary receiver and of the interference link between the secondary transmitter and the primary receiver are denoted by z_s and z_{sp}, respectively as illustrated in Fig. 1. The secondary transmitter is assumed to have perfect knowledge of z_s and z_{sp}. In particular, the secondary receiver can estimate z_s and then send it back to the secondary transmitter through an error-free feedback link. Also, the knowledge of interference channel power gain z_{sp} can be obtained by several methods: direct channel feedback from the primary receiver to the secondary transmitter [27], indirect feedback from a third party such as band manager [28], or periodic sensing of a pilot symbol sent from the primary receiver by assuming channel reciprocity [29].

The channel between the secondary transmitter and the secondary receiver is assumed to be flat-fading. Hence, under these assumptions, the discrete-time channel input-output relation is given by

$$y[i] = h_s[i]x[i] + n_w[i] + n_p[i] \quad i = 1, 2, \dots \tag{1}$$

where i represents the time index, $x[i]$ and $y[i]$ denote the transmitted and received signals, respectively, $n_w[i]$ is a zero-mean, circularly symmetric, additive complex Gaussian noise at secondary receiver, i.e., $n_w \sim \mathcal{CN}(0, \sigma_w^2)$ and $n_p[i]$ is the interference at secondary receiver due to primary user transmission. It is further assumed that $n_p[i]$ follows a Gaussian distribution, i.e., $n_w \sim \mathcal{CN}(0, \sigma_p^2)$. Thus, $n_w + n_p \sim \mathcal{CN}(0, \sigma_w^2 + \sigma_p^2)$. Without loss of generality, the variance $\sigma_w^2 + \sigma_p^2$ is assumed to be 1. Also, $\{n_w[i]\}$ and $\{n_p[i]\}$ are assumed to form an independent and identically distributed (i.i.d) sequence. In the above expression, $h_s[i]$ represents the channel fading coefficient between the secondary transmitter and the secondary receiver, and hence the channel power gain is $z_s[i] = |h_s[i]|^2$.

Hereafter, time index i is omitted for brevity of notation. We express the transmitted signal x as

$$x = \sqrt{P(z_s, z_{sp})}s \tag{2}$$

where s is a unit-power arbitrarily-distributed input signal and $P(z_s, z_{sp})$ denotes the instantaneous transmission power, which is a function of the channel gains z_s and z_{sp}. Then, by also assuming that the channel phase rotations are offset at the receiver with the knowledge of the phase of the fading coefficient h_s, the received signal in (1) can be rewritten as

$$y = \sqrt{P(z_s, z_{sp})z_s}s + w. \tag{3}$$

Let us define the input-output mutual information $\mathcal{I}(\rho)$ as

$$\mathcal{I}(\rho) = \mathcal{I}\left(s; \sqrt{\rho}s + w\right) \tag{4}$$

where $\rho = P(z_s, z_{sp})z_s$. In the case of Gaussian-distributed s, $\mathcal{I}(\rho) = \log_2(1 + \rho)$. On the other hand, for any arbitrarily distributed equiprobable signal s with a constellation $\mathcal{X}$, we have [22]

$$\mathcal{I}(\rho) = \log_2 |\mathcal{X}| - \frac{1}{\pi|\mathcal{X}|} \times \sum_{s\in\mathcal{X}} \int \log_2\left(\sum_{s'\in\mathcal{X}} \mathrm{e}^{-\rho|s-s'|^2 - 2\sqrt{\rho}\mathcal{R}\{(s-s')^* w\}}\right) \mathrm{e}^{-|w|^2} dw \tag{5}$$

where $|\mathcal{X}|$ denotes the size of the constellation $\mathcal{X}$, and the integration is carried out on the complex plane. The relation between the mutual information and the minimum mean-square error (MMSE) is given by [23]

$$\dot{\mathcal{I}}(\rho) = \mathrm{MMSE}(\rho) \log_2 \mathrm{e} \tag{6}$$

where $\dot{\mathcal{I}}(\cdot)$ denotes the first derivative of the mutual information, $\mathcal{I}(\rho)$, with respect to ρ. The above relation is a key factor in deriving the power control policy in independent and parallel channels [22]. The MMSE estimate of s is expressed as

$$\hat{s}(y, \rho) = \mathbb{E}\left\{s \mid \sqrt{\rho}s + w\right\}. \tag{7}$$

Then, the corresponding MMSE is

$$\mathrm{MMSE}(\rho) = \mathbb{E}\left\{|s - \hat{s}(y,\rho)|^2\right\}. \tag{8}$$

It should be noted that $\mathrm{MMSE}(\cdot) \in [0,1]$. When the input signal s is Gaussian, $\mathrm{MMSE}(\rho) = \frac{1}{1+\rho}$. On the other hand, for any equiprobable input signal s belonging to the constellation $\mathcal{X}$, we have [22]

$$\mathrm{MMSE}(\rho) = 1 - \frac{1}{\pi|\mathcal{X}|}\int \frac{\left|\sum_{s\in\mathcal{X}} s\mathrm{e}^{2\sqrt{\rho}\mathcal{R}\{ys^*\}-\rho|s|^2}\right|^2}{\sum_{s\in\mathcal{X}} \mathrm{e}^{2\sqrt{\rho}\mathcal{R}\{ys^*\}-\rho|s|^2}}\mathrm{e}^{-|y|^2}dy. \tag{9}$$

The above MMSE expression can be explicitly determined for specific constellations such as binary phase-shift keying (BPSK), quadrature phase-shift keying (QPSK) in the following [22]:

$$\mathrm{MMSE}^{\mathrm{BPSK}}(\rho) = 1 - \int_{-\infty}^{\infty} \tanh(2\sqrt{\rho}\phi)\frac{\mathrm{e}^{-(\phi-\sqrt{\rho})^2}}{\sqrt{\pi}}d\phi, \tag{10}$$

$$\mathrm{MMSE}^{\mathrm{QPSK}}(\rho) = \mathrm{MMSE}^{\mathrm{BPSK}}\left(\frac{\rho}{2}\right). \tag{11}$$

In addition, MMSE for 4-pulse amplitude modulation (4-PAM) is given in (12), shown at the bottom of the page. Exploiting the MMSE expression of 4-PAM in (12), MMSE for 16-quadrature amplitude modulation (16-QAM) can easily be found as follows:

$$\mathrm{MMSE}^{\text{16-QAM}}(\rho) = \mathrm{MMSE}^{\text{4-PAM}}\left(\frac{\rho}{2}\right). \tag{13}$$

For other constellations, the MMSE expression in (9) and the mutual information in (5) can easily be computed by first expressing them as double integrals and then applying the Gauss-Hermite quadrature rules [30].

III. Optimal Power Control

In this section, we derive the optimal power control policies that maximize the achievable rates of the secondary user with arbitrary input distributions subject to transmit power and interference power constraints. For a given power control policy $P(z_s, z_{sp})$, the achievable rate of the secondary user is expressed as

$$\begin{aligned}&\mathbb{E}\left\{\mathcal{I}\left(P(z_s,z_{sp})z_s\right)\right\}\\ &= \int_{z_s>0}\int_{z_{sp}>0} \mathcal{I}\left(P(z_s,z_{sp})z_s\right) f_{z_s}(z_s) f_{z_{sp}}(z_{sp}) dz_s dz_{sp}\end{aligned} \tag{14}$$

where $f_{z_s}(\cdot)$ and $f_{z_{sp}}(\cdot)$ denote the probability density functions (PDFs) of the channel gains of the transmission link between the secondary transmitter and the secondary receiver and of the interference link between the secondary transmitter and the primary receiver, respectively. With this characterization, the optimal power adaptation problem can be formulated as

$$P^*(z_s, z_{sp}) = \underset{P(z_s,z_{sp})\in\mathcal{P}}{\arg\max}\ \mathbb{E}\left\{\mathcal{I}\left(P(z_s,z_{sp})z_s\right)\right\} \tag{15}$$

where $P^*(z_s, z_{sp})$ denotes the optimal power control strategy and $\mathcal{P}$ is the set of feasible power control schemes with which the transmit power and interference power constraints are satisfied. In the following subsections, the optimization problem in (15) is studied under four scenarios, where different combinations of peak/average transmit power and peak/average interference power constraints are imposed.

A. Peak Transmit Power and Peak Interference Power Constraints

In this case, peak constraints are imposed on the transmission and interference powers, and hence the optimization problem in (15) is subject to

$$P(z_s, z_{sp}) \le P_{\mathrm{pk}}, \tag{16}$$

$$P(z_s, z_{sp}) z_{sp} \le Q_{\mathrm{pk}}, \tag{17}$$

where P_{pk} denotes the peak transmit power limit of the secondary transmitter due to hardware and battery constraints, and Q_{pk} represents the peak limit on the received interference power at the primary receiver, which is imposed to satisfy short-term QoS requirements of the primary users. The above constraints can be more concisely expressed as $P(z_s, z_{sp}) \le \min\left(P_{\mathrm{pk}}, \frac{Q_{\mathrm{pk}}}{z_{sp}}\right)$. Moreover, the objective function in (15) is strictly concave [22]. Hence, the maximum rate is achieved when the secondary user transmits at the maximum available instantaneous power. Therefore, the optimal power control is given by

$$P^*(z_{sp}) = \min\left(P_{\mathrm{pk}}, \frac{Q_{\mathrm{pk}}}{z_{sp}}\right) \tag{18}$$

which can further be written as

$$P^*(z_{sp}) = \begin{cases} \frac{Q_{\mathrm{pk}}}{z_{sp}}, & z_{sp} \ge \frac{Q_{\mathrm{pk}}}{P_{\mathrm{pk}}} \\ P_{\mathrm{pk}}, & z_{sp} < \frac{Q_{\mathrm{pk}}}{P_{\mathrm{pk}}}. \end{cases} \tag{19}$$

It should be noted that $P^*(z_{sp})$ becomes independent of the channel power gain of the transmission link z_s and the input distribution, and depends only on the channel power gain of the interference link, z_{sp}.

$$\mathrm{MMSE}^{\text{4-PAM}}(\rho) = 1 - \int_{-\infty}^{\infty} \frac{\left(\mathrm{e}^{-8\rho/5}\sinh\left(6\sqrt{\frac{\rho}{5}}\phi\right) + \sinh\left(2\sqrt{\frac{\rho}{5}}\phi\right)\right)^2}{\mathrm{e}^{-8\rho/5}\cosh\left(6\sqrt{\frac{\rho}{5}}\phi\right) + \cosh\left(2\sqrt{\frac{\rho}{5}}\phi\right)} \frac{\mathrm{e}^{-\phi^2-\rho/5}}{10\sqrt{\pi}} d\phi \tag{12}$$

B. Peak Transmit Power and Average Interference Power Constraints

In this case, the constraints are given by

$$P(z_s, z_{sp}) \leq P_{\rm pk}, \tag{20}$$

$$\mathbb{E}\left\{P(z_s, z_{sp}) z_{sp}\right\} \leq Q_{\rm avg}, \tag{21}$$

where $Q_{\rm avg}$ represents the average received interference power limit at the primary receiver, which is imposed to satisfy the long-term QoS requirements of the primary users. In the following result, we identify the optimal power adaptation strategy for this case.

Theorem 1: The optimal power control policy under the constraints in (20) and (21) is given by

$$P^*(z_s, z_{sp}) = \min\left\{\frac{1}{z_s}\text{MMSE}^{-1}\left(\min\left\{1, \frac{\lambda z_{sp}}{\log_2 \mathrm{e}\, z_s}\right\}\right), P_{\rm pk}\right\} \tag{22}$$

where $\text{MMSE}^{-1}(\cdot) \in [0, \infty)$ denotes inverse MMSE function and λ is the Lagrange multiplier, which can be determined by satisfying the average interference power constraint in (21) with equality.

Proof: See Appendix A.

The projected subgradient method is employed to numerically find the value of λ. In this method, λ is updated iteratively in the direction of a negative subgradient of the Lagrangian $L(P(z_s, z_{sp})$ given in (55) in Appendix A until convergence as follows:

$$\lambda^{(n+1)} = \left(\lambda^{(n)} - t\left(Q_{\rm avg} - \mathbb{E}\left\{P^*(z_s, z_{sp}) z_{sp}\right\}\right)\right)^+ \tag{23}$$

where $(x)^+ = \max\{0, x\}$, n is the iteration index and t is the step size. For a constant t, it was shown that convergence to the optimal λ value is guaranteed within a small range [31].

From (22), it is observed that the optimal power control policy depends on the input distribution through the inverse MMSE function. In real-time systems, $\text{MMSE}^{-1}(.)$ can be precomputed and stored in memory for the constellation of interest. Alternatively, by using the fact that MMSE is a monotonically decreasing function, $P^*(z_s, z_{sp})$ can be efficiently determined by first computing the MMSE in (9) for the corresponding input constellation and then solving for the condition in (59) in Appendix A with numerical root finding methods, e.g., bisection method. The optimal power control algorithm for this scenario is given in Table I.

The authors in [22] proposed the optimal power allocation scheme called *mercury/waterfilling* for parallel channels with arbitrary input distributions subject to an average power constraint in a non-cognitive context. Different from [22], [24], the proposed optimal power control policy in (22) is a function of the channel power gains of both transmission and interference links, z_s and z_{sp}, respectively. Therefore, we call this power control scheme as *two-dimensional truncated mercury/waterfilling*.

Remark 1: When the input signal is Gaussian, we have $\text{MMSE}^{-1}(\rho) = \frac{1}{\rho} - 1$. Substituting this expression into (22), we can see that the optimal power control policy becomes

$$P^*(z_s, z_{sp}) = \min\left\{\left(\frac{\log_2 \mathrm{e}}{\lambda z_{sp}} - \frac{1}{z_s}\right)^+, P_{\rm pk}\right\} \tag{24}$$

which is in agreement with the result obtained in [16]. It is also seen that the above power adaptation is in the form of *truncated waterfilling* with water level $\frac{\log_2 \mathrm{e}}{\lambda z_{sp}}$, which depends on the channel power gain of the interference link, z_{sp}.

TABLE I
THE OPTIMAL POWER CONTROL ALGORITHM

Algorithm 1 The optimal power control algorithm that maximizes the achievable rate of the secondary user under peak transmit power and average interference power constraints

Initialize $P_h(z_s, z_{sp}) = P_{h,\text{init}}$, $P_l(z_s, z_{sp}) = P_{l,\text{init}}$, $\epsilon > 0$, $\delta > 0$, $t > 0$, $\lambda^{(0)} = \lambda_{\text{init}}$, $\mu^{(0)} = \mu_{\text{init}}$
$n \leftarrow 0$
If the average interference constraint in (21) is satisfied when $P^*(z_s, z_{sp}) = P_{\rm pk}$, then stop.
repeat
  if $\frac{\log_2 \mathrm{e}\ z_s}{z_{sp}} \leq \lambda^{(n)}$ **then**
    $P^*(z_s, z_{sp}) = 0$
  else
    repeat
      update $P^*(z_s, z_{sp}) = \frac{1}{2}\left(P_h(z_s, z_{sp}) + P_l(z_s, z_{sp})\right)$
      if $g(P^*(z_s, z_{sp}))g(P_h(z_s, z_{sp})) < 0$ (where $g(.)$ is defined in (59)), then
        $P_l(z_s, z_{sp}) \leftarrow P^*(z_s, z_{sp})$
      else if $g(P^*(z_s, z_{sp}))g(P_l(z_s, z_{sp})) < 0$, then
        $P_h(z_s, z_{sp}) \leftarrow P^*(z_s, z_{sp})$
      end if
    until $|g(P^*(z_s, z_{sp}))| < \epsilon$
  end if
  $P^*(z_s, z_{sp}) = \max\left(P_{\rm pk}, P^*(z_s, z_{sp})\right)$
  update λ using the projected subgradient method as follows
  $\lambda^{(n+1)} = \left(\lambda^{(n)} - t(Q_{\rm avg} - \mathbb{E}\{P^*(z_s, z_{sp}) z_{sp}\})\right)^+$
  $n \leftarrow n + 1$
until $|\lambda^{(n)}(Q_{\rm avg} - \mathbb{E}\{P^*(z_s, z_{sp}) z_{sp}\})| \leq \delta$

C. Average Transmit Power and Peak Interference Power Constraints

In this case, we have the following two constraints for the optimization problem given in (15):

$$\mathbb{E}\left\{P(z_s, z_{sp})\right\} \leq P_{\rm avg}, \tag{25}$$

$$P(z_s, z_{sp}) z_{sp} \leq Q_{\rm pk}, \tag{26}$$

where $P_{\rm avg}$ denotes the average transmit power limit at the secondary transmitter. Under these constraints, the optimal power control scheme is determined as in the following result.

Theorem 2: The optimal power control policy subject to the constraints in (25) and (26) is obtained as

$$P^*(z_s, z_{sp}) = \min\left\{\frac{1}{z_s}\text{MMSE}^{-1}\left(\min\left\{1, \frac{\mu}{\log_2 \mathrm{e}\, z_s}\right\}\right), \frac{Q_{\rm pk}}{z_{sp}}\right\} \tag{27}$$

Above, the Lagrange multiplier μ is chosen such that the average transmit power constraint in (25) is satisfied with equality.

Proof: See Appendix B.

Again, the power control algorithm for this case is detailed in Table II.

TABLE II
THE OPTIMAL POWER CONTROL ALGORITHM

Algorithm 2 The optimal power control algorithm that maximizes the achievable rate of the secondary user under average transmit power and peak interference power constraints

Initialize $P_h(z_s, z_{sp}) = P_{h,\text{init}}$, $P_l(z_s, z_{sp}) = P_{l,\text{init}}$, $\epsilon > 0$, $\delta > 0$, $t > 0$, $\lambda^{(0)} = \lambda_{\text{init}}$, $\mu^{(0)} = \mu_{\text{init}}$
$n \leftarrow 0$
If the average transmit power constraint in (25) is satisfied when $P^*(z_s, z_{sp}) = \frac{Q_{\text{pk}}}{z_{sp}}$, then stop.
repeat
  if $\log_2 \mathrm{e}\, z_s \leq \mu^{(n)}$ **then**
    $P^*(z_s, z_{sp}) = 0$
  else
    Find $P^*(z_s, z_{sp})$ by bisection method as done in Algorithm 1 where $g(.)$ is replaced by $h(.)$ given in (65).
  end if
  $P^*(z_s, z_{sp}) = \max\left(\frac{Q_{\text{pk}}}{z_{sp}}, P^*(z_s, z_{sp})\right)$
  update μ using the projected subgradient method as follows
  $\mu^{(n+1)} = \left(\mu^{(n)} - t(P_{\text{avg}} - \mathbb{E}\{P^*(z_s, z_{sp})\})\right)^+$
  $n \leftarrow n + 1$
until $|\mu^{(n)}(P_{\text{avg}} - \mathbb{E}\{P^*(z_s, z_{sp})\})| \leq \delta$

TABLE III
THE OPTIMAL POWER CONTROL ALGORITHM

Algorithm 3 The optimal power control algorithm that maximizes the achievable rate of the secondary user under average transmit power and average interference power constraints

Initialize $P_h(z_s, z_{sp}) = P_{h,\text{init}}$, $P_l(z_s, z_{sp}) = P_{l,\text{init}}$, $\epsilon > 0$, $\delta > 0$, $t > 0$, $\lambda^{(0)} = \lambda_{\text{init}}$, $\mu^{(0)} = \mu_{\text{init}}$
$n \leftarrow 0$
repeat
  if $\log_2 \mathrm{e}\, z_s - \lambda^{(n)} z_{sp} \leq \mu^{(n)}$ **then**
    $P^*(z_s, z_{sp}) = 0$
  else
    Find $P^*(z_s, z_{sp})$ by bisection method as done in Algorithm 1 where $g(.)$ is replaced by $\eta(.)$ given in (71).
  end if
  update μ and λ using the projected subgradient method as follows
  $\mu^{(n+1)} = \left(\mu^{(n)} - t(P_{\text{avg}} - \mathbb{E}\{P^*(z_s, z_{sp})\})\right)^+$
  $\lambda^{(n+1)} = \left(\lambda^{(n)} - t(Q_{\text{avg}} - \mathbb{E}\{P^*(z_s, z_{sp}) z_{sp}\})\right)^+$
  $n \leftarrow n + 1$
until $|\mu^{(n)}(P_{\text{avg}} - \mathbb{E}\{P^*(z_s, z_{sp})\})| \leq \delta$ and $|\lambda^{(n)}(Q_{\text{avg}} - \mathbb{E}\{P^*(z_s, z_{sp}) z_{sp}\})| \leq \delta$

Remark 2: Inserting $\text{MMSE}^{-1}(\rho) = \frac{1}{\rho} - 1$ into (27), the optimal power control policy becomes the *truncated waterfilling* scheme for Gaussian inputs as follows

$$P^*(z_s, z_{sp}) = \min\left\{\left(\frac{\log_2 \mathrm{e}}{\mu} - \frac{1}{z_s}\right)^+, \frac{Q_{\text{pk}}}{z_{sp}}\right\} \tag{28}$$

which has the same structure as given in [16].

D. Average Transmit Power and Average Interference Power Constraints

Finally, we consider the case in which the secondary transmitter operates under both average transmit and average interference power constraints expressed as

$$\mathbb{E}\{P(z_s, z_{sp})\} \leq P_{\text{avg}}, \tag{29}$$

$$\mathbb{E}\{P(z_s, z_{sp}) z_{sp}\} \leq Q_{\text{avg}}. \tag{30}$$

The main characterization is as follows with the power control algorithm provided in Table III:

Theorem 3: The optimal power control policy under the constraints in (29) and (30) is determined as

$$P^*(z_s, z_{sp}) = \frac{1}{z_s}\text{MMSE}^{-1}\left(\min\left\{1, \frac{\mu + \lambda z_{sp}}{\log_2 \mathrm{e}\, z_s}\right\}\right) \tag{31}$$

where μ and λ are the Lagrange multipliers, which can be jointly obtained by inserting the above optimal power expression into the constraints given in (29) and (30).

Proof: See Appendix C.

Remark 3: When the input signal is Gaussian, we have

$$P^*(z_s, z_{sp}) = \left(\frac{\log_2 \mathrm{e}}{\mu + \lambda z_{sp}} - \frac{1}{z_s}\right)^+ \tag{32}$$

which is again consistent with the power allocation scheme given in [16].

Overall, our results throughout this section can be regarded as the generalization of the optimal power control strategies characterized for only Gaussian inputs to arbitrarily distributed inputs, including frequently-used finite constellations such as BPSK, QPSK, and QAM.

IV. LOW-POWER REGIME ANALYSIS

In this section, we characterize the optimal power control policies that maximize the achievable rates of the secondary user with arbitrary input distributions in the low-power regime. We note that operating at low power levels is of interest in cognitive radio systems due to the facts that less interference is inflicted on the primary users and energy efficiency of cognitive secondary users is generally improved in this regime.

Similarly as in the previous section, the proposed optimal power expressions are derived for general fading distributions. In special cases, we further provide closed-form approximations of the maximum achievable rates in the low-power regime. In determining these expressions, we consider unit-mean Nakagami-m fading, which is analytically tractable and widely used to model urban and indoor multipath propagation. By changing the parameter $m \in [0.5, \infty)$, the Nakagami-m fading covers different models describing the statistical behavior of the radio propagation environment. More specifically, in the case of $m = 0.5$, the Nakagami-m distribution specializes to the one-sided Gaussian distribution, which corresponds to the most severe fading. For $m = 1$, the Nakagami-m distribution becomes the Rayleigh fading, which is used to model multipath fading with no direct line-of-sight (LOS) component. As m goes to infinity, the Nakagami-m fading channel converges to a non-fading additive white Gaussian noise (AWGN) channel. Under the assumption of the Nakagami-m fading, the channel power gains of the transmission link, z_s, and interference link, z_{sp}, follow gamma distributions with PDFs given, respectively, as

$$f_{z_s}(z_s; m_s) = \frac{m_s^{m_s} z_s^{m_s - 1}}{\Gamma(m_s)} \mathrm{e}^{-m_s z_s} \qquad z_s \geq 0, m_s \geq 0.5, \tag{33}$$

$$f_{z_{sp}}(z_{sp}; m_{sp}) = \frac{m_{sp}^{m_{sp}} z_{sp}^{m_{sp} - 1}}{\Gamma(m_{sp})} \mathrm{e}^{-m_{sp} z_{sp}} \quad z_{sp} \geq 0, m_{sp} \geq 0.5 \tag{34}$$

where $\Gamma(.)$ is the gamma function [32, eq. 6.1.1] and m_s and m_{sp} control the severity of the amplitude fading of the transmission link and the interference link, respectively.

A. Peak Transmit Power and Peak Interference Power Constraints

The optimal power policy in the low power regime subject to the constraints in (16) and (17) is the same as in (18). Next, we find a closed-form expression for the maximum achievable rate of the secondary user attained with the optimal power control policy in (18).

We first express the mutual information achieved with arbitrary input distributions in the low-power regime as follows:

$$\mathcal{I}(\rho) = \dot{\mathcal{I}}(0)\rho \log_2 \mathrm{e} + \frac{\ddot{\mathcal{I}}(0)}{2}\rho^2 \log_2 \mathrm{e} + o(\rho^2) \tag{35}$$

where $\rho = P(z_s, z_{sp})z_s$ and $\dot{\mathcal{I}}(0) = 1$ [22]. Substituting the optimal power control policy in (18) into the above mutual information expression and taking the expectation with respect to fading, the maximum achievable rate can be found as in (36), shown at the bottom of the page.

Evaluating the integrals in (36) gives the closed-form expression for the maximum achievable rate in (37), shown at the bottom of the page, where $\Gamma(a, b)$ is the incomplete gamma function [32, eq. 6.5.3].

In addition, if the power allocation problem is only constrained by peak transmit power constraint P_{pk}, the achievable rate can be computed in (38), shown at the bottom of the page. Evaluating the integral in (38) yields the closed-form achievable rate expression under only P_{pk} constraint in the following:

$$R_{\mathrm{opt}}(P_{\mathrm{pk}}) = \left(P_{\mathrm{pk}} \frac{\Gamma(m_s+1)}{\Gamma(m_s)m_s} + \ddot{\mathcal{I}}(0)\frac{P_{pk}^2}{2}\frac{\Gamma(m_s+2)}{\Gamma(m_s)m_s^2} \right) \log_2 \mathrm{e}. \tag{39}$$

Moreover, if the power allocation problem is only constrained by peak interference power constraint Q_{pk}, the achievable rate can be expressed in (40), shown at the bottom of the page. By performing the integration in (40), a closed-form achievable rate expression subject to only Q_{pk} constraint can be found as

$$\begin{aligned} R_{\mathrm{opt}}(Q_{\mathrm{pk}}) = {} & Q_{\mathrm{pk}} \left(\frac{m_{sp}}{m_s}\right) \frac{\Gamma(m_s+1)\Gamma(m_{sp}-1)}{\Gamma(m_{sp})\Gamma(m_s)} \log_2 \mathrm{e} \\ & + \frac{Q_{\mathrm{pk}}^2}{2}\ddot{\mathcal{I}}(0)\left(\frac{m_{sp}}{m_s}\right)^2 \frac{\Gamma(m_s+2)\Gamma(m_{sp}-2)}{\Gamma(m_{sp})\Gamma(m_s)} \log_2 \mathrm{e}. \end{aligned} \tag{41}$$

B. Peak Transmit Power and Average Interference Power Constraints

In this case, by using the low-power expansion of MMSE in terms of the first and second derivatives of the mutual information, we can simplify the optimal power control policy in the low power regime as in the following result.

Theorem 4: The optimal power control policy that maximizes the achievable rate of the secondary user in the low-power

$$\begin{aligned} R_{\mathrm{opt}}(P_{\mathrm{pk}}, Q_{\mathrm{pk}}) = {} & \int_0^{\frac{Q_{\mathrm{pk}}}{P_{\mathrm{pk}}}} \int_0^{\infty} \left(P_{\mathrm{pk}} z_s + \frac{\ddot{\mathcal{I}}(0) P_{\mathrm{pk}}^2 z_s^2}{2} \right) \log_2 \mathrm{e}\, f_{z_s}(z_s) f_{z_{sp}}(z_{sp}) dz_s dz_{sp} \\ & + \int_{\frac{Q_{\mathrm{pk}}}{P_{\mathrm{pk}}}}^{\infty} \int_0^{\infty} \left(\frac{Q_{\mathrm{pk}} z_s}{z_{sp}} + \frac{\ddot{\mathcal{I}}(0) Q_{\mathrm{pk}}^2}{2} \frac{z_s^2}{z_{sp}^2} \right) \log_2 \mathrm{e}\, f_{z_s}(z_s) f_{z_{sp}}(z_{sp}) dz_s dz_{sp} \end{aligned} \tag{36}$$

$$\begin{aligned} R_{\mathrm{opt}}(P_{\mathrm{pk}}, Q_{\mathrm{pk}}) = {} & \left(P_{\mathrm{pk}} \frac{\Gamma(m_s+1)}{\Gamma(m_s)m_s} + \ddot{\mathcal{I}}(0)\frac{P_{\mathrm{pk}}^2}{2}\frac{\Gamma(m_s+2)}{\Gamma(m_s)m_s^2} \right) \left(1 - \frac{\Gamma\left(m_{sp}, \frac{m_{sp}Q_{\mathrm{pk}}}{P_{\mathrm{pk}}}\right)}{\Gamma(m_{sp})} \right) \log_2 \mathrm{e} + Q_{\mathrm{pk}} \frac{m_{sp}}{m_s} \frac{\Gamma(m_s+1)}{\Gamma(m_s)} \\ & \times \frac{\Gamma\left(m_{sp}-1, \frac{m_{sp}Q_{\mathrm{pk}}}{P_{\mathrm{pk}}}\right)}{\Gamma(m_{sp})} \log_2 \mathrm{e} + \ddot{\mathcal{I}}(0)\frac{Q_{\mathrm{pk}}^2}{2}\left(\frac{m_{sp}}{m_s}\right)^2 \frac{\Gamma(m_s+2)}{\Gamma(m_s)} \frac{\Gamma\left(m_{sp}-2, \frac{m_{sp}Q_{\mathrm{pk}}}{P_{\mathrm{pk}}}\right)}{\Gamma(m_{sp})} \log_2 \mathrm{e} \ \text{ for } \ m_{sp} > 2 \end{aligned} \tag{37}$$

$$R_{\mathrm{opt}}(P_{\mathrm{pk}}) = \int_0^{\infty} \int_0^{\infty} \left(P_{\mathrm{pk}} z_s + \frac{\ddot{\mathcal{I}}(0) P_{\mathrm{pk}}^2 z_s^2}{2} \right) \log_2 \mathrm{e} f_{z_s}(z_s) f_{z_{sp}}(z_{sp}) dz_s dz_{sp} \tag{38}$$

$$R_{\mathrm{opt}}(Q_{\mathrm{pk}}) = \int_0^{\infty} \int_0^{\infty} \left(\frac{Q_{\mathrm{pk}} z_s}{z_{sp}} + \frac{\ddot{\mathcal{I}}(0) Q_{\mathrm{pk}}^2}{2} \frac{z_s^2}{z_{sp}^2} \right) \log_2 \mathrm{e} f_{z_s}(z_s) f_{z_{sp}}(z_{sp}) dz_s dz_{sp} \tag{40}$$

regime, i.e., as $P_{\mathrm{pk}} \to 0$ and $Q_{\mathrm{avg}} \to 0$, with arbitrary input distributions belonging to discrete constellations under the constraints in (20) and (21) can be approximated as

$$P^*(z_s, z_{sp}) = \min\left\{ \left(\frac{\frac{\lambda z_{sp}}{\log_2 \mathrm{e}} - z_s}{\ddot{\mathcal{I}}(0) z_s^2} \right)^+, P_{\mathrm{pk}} \right\} \tag{42}$$

where $\ddot{\mathcal{I}}(0)$ denotes the second derivative of mutual information evaluated at SNR $= 0$ and λ is the Lagrange multiplier associated with the average interference power constraint in (21).

Proof: See Appendix D.

We immediately see that the resulting optimal power control policy in (42) is simpler and depends on the input distribution through $\ddot{\mathcal{I}}(0)$ rather than MMSE$^{-1}(\cdot)$. In particular, for quadrature symmetric constellations such as QPSK, 8-PSK or 16-QAM, we have $\ddot{\mathcal{I}}(0) = -1$ while real valued constellations such as BPSK and m-PAM have $\ddot{\mathcal{I}}(0) = -2$ [22]. It should also be noted that we can obtain the low power behavior of MMSE for the Gaussian input by setting $\ddot{\mathcal{I}}(0) = -1$ in (72). Hence, inserting $\ddot{\mathcal{I}}(0) = -1$ in (42), the optimal power expressions for Gaussian input can readily be obtained.

C. Average Transmit Power and Peak Interference Power Constraints

Similarly as in the previous subsection, we first identify the optimal power adaptation strategy in the low-power regime.

Theorem 5: In the low-power regime, the optimal power control policy subject to the constraints in (25) and (26) is approximated by

$$P^*(z_s, z_{sp}) = \min\left\{ \left(\frac{\frac{\mu}{\log_2 \mathrm{e}} - z_s}{\ddot{\mathcal{I}}(0) z_s^2} \right)^+, \frac{Q_{\mathrm{pk}}}{z_{sp}} \right\}. \tag{43}$$

Since similar procedures as in the proof of Theorem 4 are employed, the proof is omitted. Inserting the above optimal power policy into (35) and taking the expectation with respect to channel power gains z_s and z_{sp} do not yield a closed-form maximum achievable rate expression. Hence, we provide closed-form expressions under only an average transmit power constraint.

If only an average power constraint is imposed (or if the interference constraint is loose), the optimal power control has the same formulation as in (43) with $\frac{Q_{\mathrm{pk}}}{z_{sp}}$ eliminated. Hence, in this setting, the maximum achievable rate can be found as

$$R_{\mathrm{opt}}(P_{\mathrm{avg}}) = \int_{\frac{\mu}{\log_2 \mathrm{e}}}^{\infty} \frac{1}{2\ddot{\mathcal{I}}(0)} \left(\left(\frac{\mu}{\log_2 \mathrm{e}\, z_s} \right)^2 - 1 \right) \log_2 \mathrm{e}\, f_{z_s}(z_s) dz_s \tag{44}$$

and the above integration yields the following closed-form maximum achievable rate expression:

$$R_{\mathrm{opt}}(P_{\mathrm{avg}}) = \frac{\mu^2 m_s^2}{2\ddot{\mathcal{I}}(0) \log_2 \mathrm{e}} \left(\frac{\Gamma\left(m_s - 2, \frac{m_s \mu}{\log_2 \mathrm{e}}\right)}{\Gamma(m_s)} \right) - \frac{\log_2 \mathrm{e}}{2\ddot{\mathcal{I}}(0)} \left(\frac{\Gamma\left(m_s, \frac{m_s \mu}{\log_2 \mathrm{e}}\right)}{\Gamma(m_s)} \right). \tag{45}$$

If the average transmit power constraint in (25) is satisfied with strict inequality, then μ is zero. Otherwise, μ is determined by satisfying the constraint in (25) with equality or equivalently by solving

$$\frac{\mu m_s^2}{\ddot{\mathcal{I}}(0) \log_2 \mathrm{e}} \left(\frac{\Gamma\left(m_s - 2, \frac{m_s \mu}{\log_2 \mathrm{e}}\right)}{\Gamma(m_s)} \right) - \frac{m_s}{\ddot{\mathcal{I}}(0)} \left(\frac{\Gamma\left(m_s - 1, \frac{m_s \mu}{\log_2 \mathrm{e}}\right)}{\Gamma(m_s)} \right) = P_{\mathrm{avg}}. \tag{46}$$

It should be noted that the expressions in (45) and (46) are in terms of the incomplete gamma function, which can easily be computed via numerical tools. To obtain further simplified achievable rate expressions free of the Lagrange multiplier μ, we further approximate and simplify the formulations in (45) and (46) at asymptotically low power levels by using the fact that

$$\lim_{P_{\mathrm{avg}} \to 0} \mu(P_{\mathrm{avg}}) = \infty \tag{47}$$

which can be shown by following the approach below. Let us first define the function $H(x)$ for $x \in (0, \infty)$ as follows:

$$H(x) = \mathbb{E}\left[\frac{1}{z_s} \mathrm{MMSE}^{-1}\left(\min\left\{ 1, \frac{x}{\log_2 \mathrm{e}\, z_s} \right\} \right) \right] \tag{48}$$

which is continuous, takes nonnegative values by definition, and strictly monotonically decreasing since it is the inverse of the MMSE function, which is also strictly monotonically decreasing in its argument. Hence, the function $H(x)$ is invertible by construction. The Lagrange multiplier $\mu(P_{\mathrm{avg}})$ is a function of P_{avg} and can be found by setting $H(\mu(P_{\mathrm{avg}})) = P_{\mathrm{avg}}$. Taking the limits of both sides as P_{avg} goes to zero and using the above-mentioned properties of the function $H(x)$, the relation in (47) is obtained.

Consequently, we perform series expansion for expressions in (45) and (46) as $\mu(P_{\mathrm{avg}}) \to \infty$ as follows:

$$R_{\mathrm{opt}}(P_{\mathrm{avg}}) = \frac{2^{-m_s \mu} \mu^{m_s}}{2\ddot{\mathcal{I}}(0)\Gamma(m_s)} \left(-\frac{2 m_s^{m_s - 2} \log(2)^{m_s - 3}}{\mu^2} + o\left(\frac{1}{\mu}\right)^3 \right) \tag{49}$$

$$P_{\mathrm{avg}} = \frac{2^{-m_s \mu} \mu^{m_s}}{\ddot{\mathcal{I}}(0)\Gamma(m_s)} \left(-\frac{m_s^{m_s - 2} \log(2)^{m_s - 3}}{\mu^3} + o\left(\frac{1}{\mu}\right)^4 \right). \tag{50}$$

By combining the above expressions, we can rewrite $R_{\mathrm{opt}}(P_{\mathrm{avg}})$ in terms of P_{avg} as

$$R_{\mathrm{opt}}(P_{\mathrm{avg}}) = P_{\mathrm{avg}} \mu(P_{\mathrm{avg}}). \tag{51}$$

By solving the expression in (50), $\mu(P_{\mathrm{avg}})$ can be found as

$$\mu(P_{\mathrm{avg}}) = \frac{3 - m_s}{m_s \log(2)} W_{-1}\left(\beta \left(\frac{1}{P_{\mathrm{avg}}} \right)^{\frac{1}{3 - m_s}} \right) \tag{52}$$

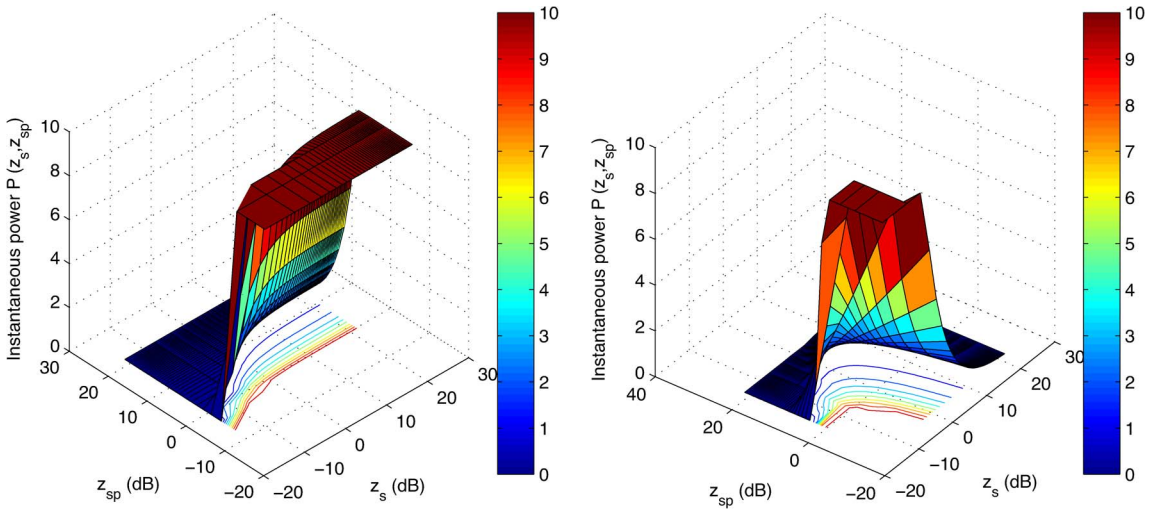

Fig. 2. Instantaneous power level vs. channel power gains z_s and z_{sp} under peak transmit and average interference power constraints. $P_{\text{pk}} = 10$ dB and $Q_{\text{avg}} = 6$ dB. Left and right subfigures are for the Gaussian and BPSK inputs, respectively.

where $m_s > 3$, $\beta = \frac{1}{3-m_s}\left(\frac{m_s}{-\ddot{\mathcal{I}}(0)\Gamma(m_s)}\right)^{\frac{1}{3-m_s}}$, which depends on the input distribution through $\ddot{\mathcal{I}}(0)$, and $W_{-1}(.)$ represents the lower branch of the Lambert function [36]. Hence, inserting $\mu(P_{\text{avg}})$ in (52) into (51) gives

$$R_{\text{opt}}(P_{\text{avg}}) = \frac{3-m_s}{m_s \log(2)} P_{\text{avg}} W_{-1}\left(\beta\left(\frac{1}{P_{\text{avg}}}\right)^{\frac{1}{3-m_s}}\right). \tag{53}$$

By substituting $\ddot{\mathcal{I}}(0) = -1$ into the above rate expression, the result can readily be specialized to the Gaussian input, which is obtained in [37], where the unit of the achievable rate is chosen as nats per channel use.

D. Average Transmit Power and Average Interference Power Constraints

Finally, we address the case in which average constraints are imposed on the transmission and interference powers, and obtain the following result on the low-power approximation of the optimal power control strategy. Again the proof is omitted for brevity.

Theorem 6: In the low-power regime, the optimal power control policy subject to the constraints in (29) and (30) is approximated by

$$P^*(z_s, z_{sp}) = \left(\frac{\frac{\mu+\lambda z_{sp}}{\log_2 \text{e}} - z_s}{\ddot{\mathcal{I}}(0) z_s^2}\right)^+, \tag{54}$$

where μ and λ are the Lagrange multipliers corresponding to the constraints given in (29) and (30), respectively.

V. Numerical Results

In this section, we first provide numerical results to identify the impact of transmit power and interference power constraints, input distributions, and fading severity on the achievable rates attained with optimal power control. Subsequently, we analyze the optimal power control in the low-power regime. In the optimization algorithm, unless mentioned explicitly, we set $\epsilon = 0.00001$, $\delta = 0.0001$, $t = 0.01$ in the iterations. In the numerical results, we consider Nakagami-m fading.

A. Optimal Power Control

In Fig. 2, we plot the instantaneous power levels as a function of the channel power gains of the transmission link z_s and of the interference link z_{sp}, respectively, for the Gaussian signal (left subfigure) and BPSK signal (right subfigure). Peak transmit power and average interference power constraints are imposed with $P_{\text{pk}} = 10$ dB and $Q_{\text{avg}} = 6$ dB. When the input is Gaussian, it is seen that more power is assigned to the stronger channel (i.e., higher values of z_s) opportunistically while the power level generally diminishes as the fading power of the interference link, z_{sp}, increases. In contrast to the power adaptation scheme for the Gaussian input, it is observed that instantaneous power for BPSK signal first increases and then decreases with the channel power gain of the transmission link, z_s. In other words, when the channel gain is higher than a threshold, the transmission power is lowered with increasing channel gain. This is due to the fact that increasing the power beyond a certain level is not very beneficial because BPSK mutual information is upper bounded by 2 bits/symbol and gets saturated eventually. Hence, the strategy of performing channel inversion at very high channel gains and allocating more power to the weaker channel conditions turns out to be the optimal one. Note that this strategy has implications on interference management, highlighting the importance of addressing power control for practical input distributions in cognitive radio settings.

In Fig. 3, we plot the maximum achievable rates in bits per channel use as a function of the peak transmit power constraint P_{pk} for Gaussian, BPSK and QPSK inputs and for different values of m_s and m_{sp} (i.e., different fading severity) in the transmission and interference links. In this figure, we consider that a peak interference constraint is also imposed and Q_{pk} is

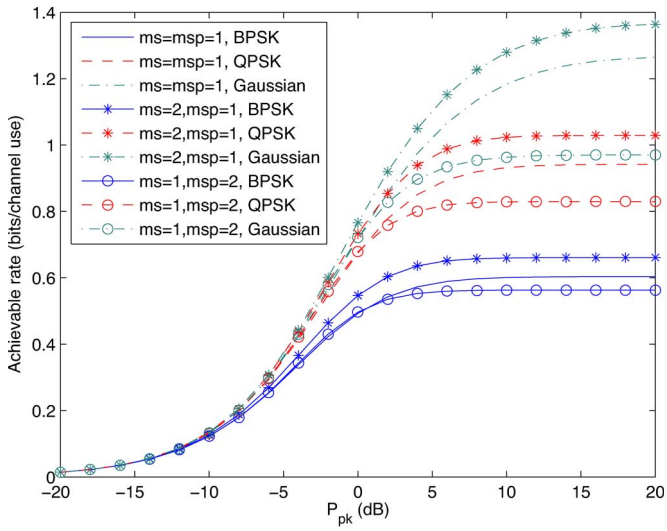

Fig. 3. Maximum achievable rate vs. peak transmit power constraint, $P_{\rm pk}$, for BPSK, QPSK, and Gaussian inputs under different fading severity. $Q_{\rm pk} = -1$ dB.

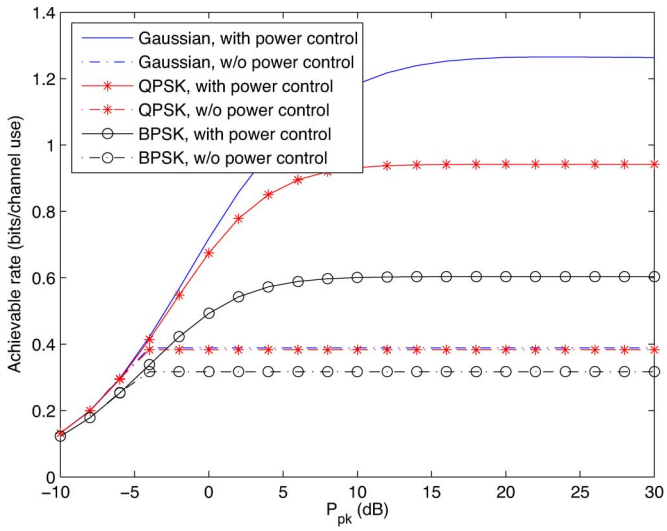

Fig. 4. Maximum achievable rate vs. peak transmit power constraint, $P_{\rm pk}$, for BPSK, QPSK, and Gaussian inputs with or without the CSI of the interference link. $Q_{\rm pk} = -1$ dB.

chosen as -1 dB. It is seen that as $P_{\rm pk}$ increases, maximum achievable rates initially increase and then stay constant for all inputs because the transmission power is eventually limited by the interference power constraint, $Q_{\rm pk}$. It is observed that Gaussian inputs always achieve higher rates compared to QPSK and BPSK inputs in the high power regime while the performances of Gaussian, QPSK and BPSK inputs approach each other in the low power regime. Another observation is that if the transmission link experiences less severe fading or the fading in the interference link is more severe, the achievable rates become higher. We also note that as the fading in the interference link becomes more severe, the increase in the maximum achievable rate of Gaussian inputs is higher than the increase in the maximum achievable rates of QPSK and BPSK inputs.

In Fig. 4, we again display the maximum achievable rates as a function of the peak transmit power limit, $P_{\rm pk}$ for Gaussian, BPSK and QPSK inputs. It is assumed that $Q_{\rm pk} = -1$ dB. In this figure, we consider two cases regarding the availability of the channel side information (CSI). When the CSI of the interference link z_{sp} is available at the transmitter, optimal transmission power is given in (19). On the other hand, in the lack of the knowledge of z_{sp}, it is assumed that the interference outage constraint $\Pr(Pz_{sp} > Q_{\rm pk}) \leq \epsilon$ is imposed, i.e., the probability that the received power exceeds the peak interference level is limited by ϵ. Hence, under this setting, the transmit power is given by $P = \min\left\{P_{\rm pk}, \frac{Q_{\rm pk}}{F^{-1}_{z_{sp}}(1-\epsilon)}\right\}$ where $F^{-1}_{z_{sp}}$ denotes the inverse cumulative distribution function (CDF) of z_{sp}. It is assumed that $\epsilon = 0.1$. It is seen that small gains are possible at low values of $P_{\rm pk}$ in the absence of the CSI of the interference link. This is due to allowing the violation of the peak interference level with some small probability. Note that violations are not tolerated when z_{sp} is perfectly known. The possible gains diminish if stricter outage constraints are imposed. On the other hand, when $P_{\rm pk}$ is relatively large, we notice that having CSI and adapting the power level benefits the secondary users. This is also beneficial to the primary users as their interference constraints are satisfied all the time. In the figure, it is also interesting to note that the throughput gains due to the availability of CSI of interference link z_{sp} is the highest for the Gaussian input, and throughput gain increases as the modulation size increases.

In Fig. 5, we plot the maximum achievable rates as a function of the average interference power constraint, $Q_{\rm avg}$ for Gaussian, 16-QAM, QPSK and BPSK inputs. In the left subfigure, peak transmit power constraint is not imposed whereas $P_{\rm pk}$ is set to 6 dB in the right subfigure. It is assumed that $m_s = m_{sp} = 1$. We both consider the achievable rates of non-Gaussian inputs (i.e.,16-QAM, QPSK and BPSK inputs) achieved with optimal power control assuming Gaussian input signaling and with the proposed power control considering the non-Gaussian signaling. When there is no peak transmit power constraint, maximum achievable rate with Gaussian input increases as $Q_{\rm avg}$ increases while maximum achievable rates of 16-QAM, QPSK and BPSK inputs increase first and then saturate at 4, 2 and 1 bit per channel use, respectively, due to being finite constellations. When the peak transmit power constraint is imposed, maximum achievable rates for all inputs increase initially with increasing $Q_{\rm avg}$ and then start saturating due to the presence of $P_{\rm pk}$ as seen in the right subfigure. It is also observed that the achievable rates of 16-QAM, QPSK and BPSK inputs obtained with the power control assuming Gaussian input signaling are lower than that obtained under the proposed optimal power control considering non-Gaussian signaling since the power control under the assumption of Gaussian input signaling is suboptimal for these non-Gaussian inputs. Therefore, it is concluded that if the actual signal input distribution is not taken into account, considerable performance loss occurs for systems optimized under the Gaussian input assumption.

In Fig. 6, we plot the maximum achievable rates as a function of the average transmit power constraint, $P_{\rm avg}$ for Gaussian, QPSK and BPSK inputs under either peak interference power

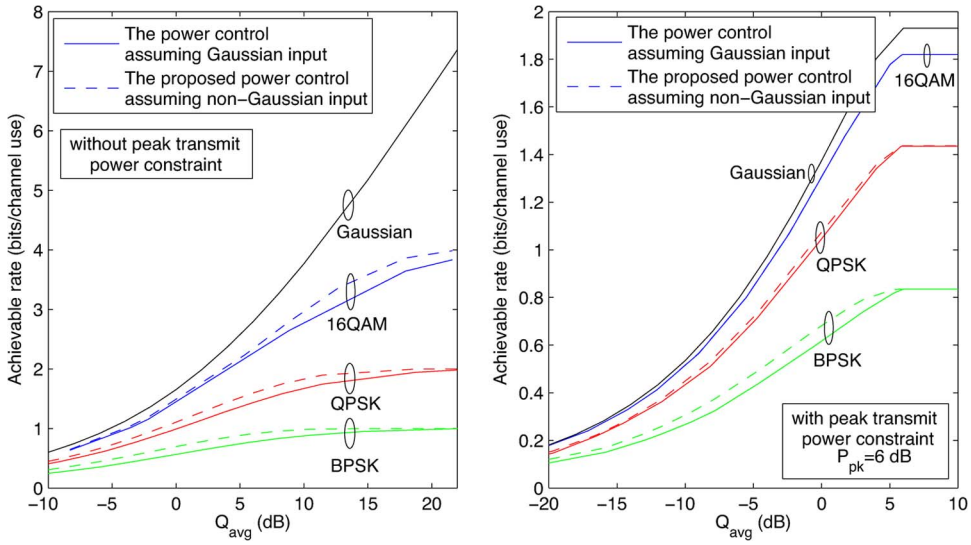

Fig. 5. Maximum achievable rate vs. average interference power constraint, $Q_{\rm avg}$, for BPSK, QPSK, 16-QAM and Gaussian inputs. While only an average interference power constraint is considered in the left subfigure, an additional peak transmit constraint with $P_{\rm pk} = 6$ dB is imposed in the right subfigure.

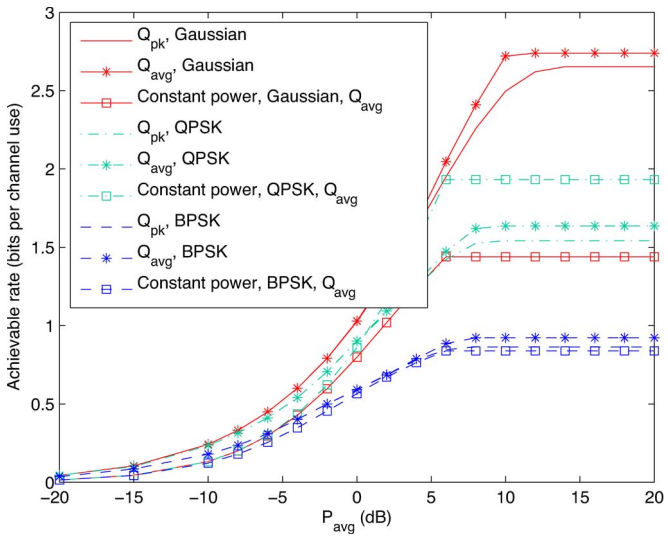

Fig. 6. Maximum achievable rate vs. average transmit power constraint, $P_{\rm avg}$, for BPSK, QPSK, and Gaussian inputs under either average or peak interference constraints, and constant power scheme.

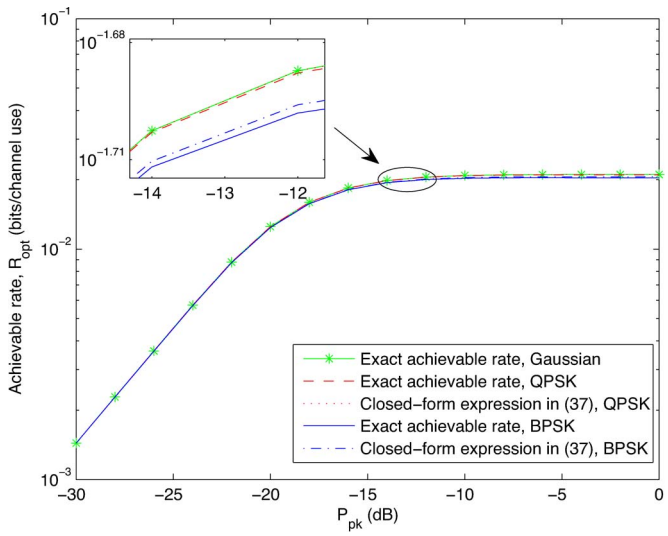

Fig. 7. Maximum achievable rate vs. peak transmit power constraint, $P_{\rm pk}$. $Q_{\rm pk} = -20$ dB.

constraint $Q_{\rm pk}$ or average interference power constraint, $Q_{\rm avg}$. It is assumed that $Q_{\rm pk} = Q_{\rm avg} = 6$ dB. To highlight the gains achieved with power control, we also plot the rates attained with constant power transmissions when $Q_{\rm avg}$ is imposed. Expectedly, higher achievable rates are observed under average interference constraints compared to that attained under peak interference constraints for all inputs since power adaptation under average interference power constraints is more flexible than that under peak interference power constraints. It is observed that the highest rate is achieved with the Gaussian input and there is substantial throughput difference between Gaussian input and BPSK, QPSK inputs. Hence if the system performance is predicted under the assumption of Gaussian input and the inputs are chosen from discrete constellations in actual applications, it is seen that there would be considerable performance loss in terms of achievable rates. It is also observed that optimal power control policy always outperforms constant power scheme for all inputs, but the highest throughput gain is achieved with Gaussian input.

B. Low-Power Analysis

Fig. 7 shows the maximum achievable rates vs. peak transmit power constraint, $P_{\rm pk}$ for Gaussian, BPSK and QPSK inputs. It is assumed that $m_s = 1, m_{sp} = 3$. In this figure, a low-power scenario is considered. As before, it is again observed that the maximum achievable rates increase with increasing $P_{\rm pk}$ and then become limited by peak interference power constraint, $Q_{\rm pk}$. It is seen that low-power approximation in (37) matches well with the exact rates, confirming the accuracy of the approximation at low power levels. It is also seen that Gaussian and QPSK inputs exhibit nearly the same performance in the

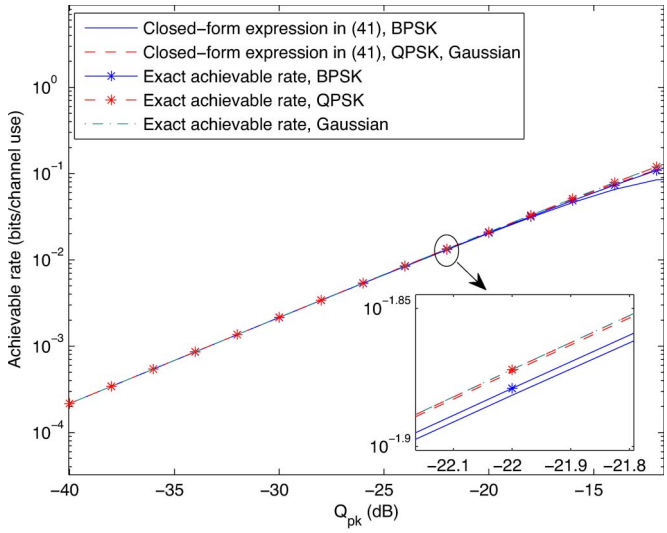

Fig. 8. Maximum achievable rate vs. peak interference power constraint, $Q_{\rm pk}$.

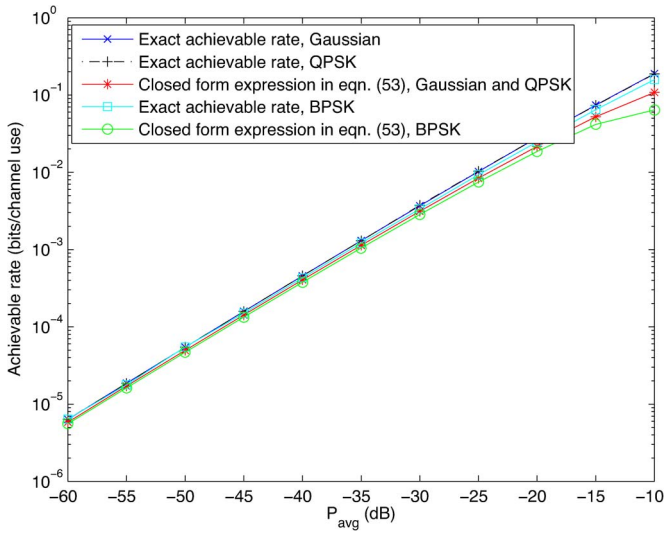

Fig. 10. Maximum achievable rate vs. average transmit power constraint, $P_{\rm avg}$.

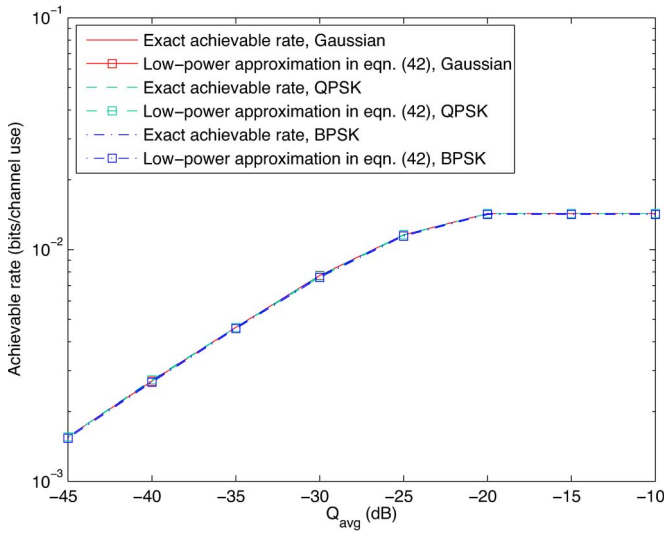

Fig. 9. Maximum achievable rate vs. average interference power constraint, $Q_{\rm avg}$. $P_{\rm pk} = -20$ dB.

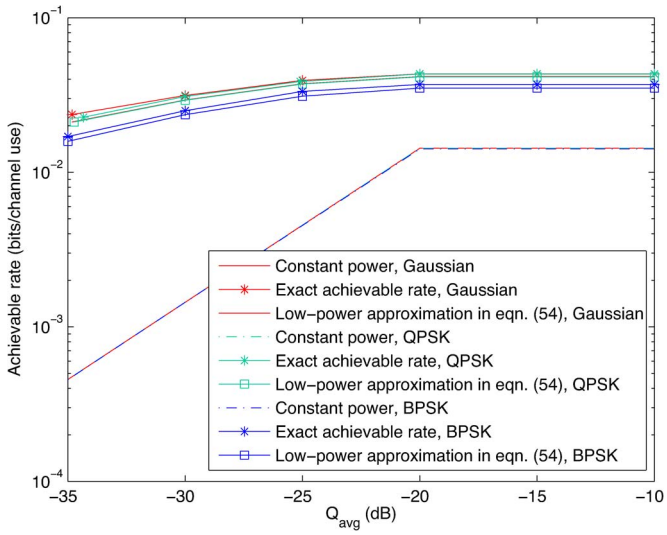

Fig. 11. Maximum achievable rate vs. average interference power constraint, $Q_{\rm avg}$. $P_{\rm avg} = -20$ dB.

low power regime. Therefore, QPSK input can be efficiently used in practical systems rather than the Gaussian input which is difficult to implement.

In Fig. 8, we display the maximum achievable rates vs. peak interference power constraint, $Q_{\rm pk}$ for Gaussian, BPSK and QPSK inputs in the low-power regime. It is again assumed that $m_s = 1, m_{sp} = 3$. The maximum achievable rates increase with increasing $Q_{\rm pk}$ for all inputs. The gap between the closed-form maximum achievable rate expression in (41) and the exact maximum achievable rate evaluated by inserting the corresponding optimal transmission power into (5) is relatively small in the low-power regime.

Fig. 9 depicts the maximum achievable rates as a function of average interference power constraint, $Q_{\rm avg}$ for Gaussian, BPSK and QPSK inputs. Again, a low-power scenario is addressed. We consider peak constraint on the transmit power, i.e., $P_{\rm pk} = -20$ dB. It is assumed that $m_s = m_{sp} = 1$. As $Q_{\rm avg}$ increases, the maximum achievable rates increase and get saturated for all inputs due to limitations on the peak transmit power, $P_{\rm pk}$. It is seen that the low-power approximation (42) of the optimal power control leads to similar performance in terms of the achievable rates compared with the optimal power control scheme, demonstrating the accuracy of (42).

In Fig. 10, we illustrate the maximum achievable rates vs. average transmit power constraint, $P_{\rm avg}$ for Gaussian, BPSK and QPSK inputs. We consider that $m_s = 4, m_{sp} = 1$. As $P_{\rm avg}$ increases, maximum achievable rates increase. It is seen that for low power values, the closed-form maximum achievable rate expression in (53) matches well with the exact maximum achievable rate achieved with the corresponding optimal transmission power in (43) without a constraint on the peak interference power. This is in agreement with our analysis in Section IV-C.

In Fig. 11, we display the maximum achievable rates vs. average interference power constraint, $Q_{\rm avg}$ for Gaussian, BPSK and QPSK inputs under optimal power control and constant

power schemes. We set $m_s = m_{sp}$ to 1 and $P_{\text{avg}} = -20$ dB. The maximum achievable rates increase with increasing Q_{avg} and then capped due to the presence of P_{avg}. It is seen that substantially higher rates are achieved with optimal power control policy compared to constant power scheme. It is observed from the figure that QPSK and Gaussian inputs show nearly the same throughput gain whereas BPSK has the smallest throughput gain when the optimal power control is applied.

VI. Conclusion

In this paper, we have obtained the optimal power control policies for underlay cognitive radio systems with arbitrary input signaling subject to peak/average transmit power and peak/average interference power constraints for general fading distributions. We have also provided low-complexity power control algorithms. In addition, we have analyzed the optimal power control policy in the low-power regime. Closed-form maximum achievable rate expressions are derived under peak transmit power, peak interference power and average transmit power constraints. Numerical results reveal that Gaussian input expectedly results in higher achievable rates at high power levels while Gaussian inputs and QPSK provide nearly the same performance in the low-power regime. Therefore, QPSK input can be efficiently used in practical systems rather than the Gaussian input which is not easy to realize. It is also shown that there can be considerable performance degradation if the system is designed under the assumption of Gaussian input and the inputs are chosen from discrete constellations at moderate and high power levels. Moreover, we have observed that power control provides significant improvements in performance when compared with that achieved with constant power transmissions. Finally, we have demonstrated that simpler low-power approximations of the power control strategies and achievable rates provide very accurate results when compared to exact expressions.

Appendix

A. Proof of Theorem 1

The objective function in (15) is strictly concave since it follows from the relation in (6) that the first derivative of the mutual information is MMSE, which is a strictly decreasing function [22]. Also, the optimization problem is subject to affine inequality constraints given in (20) and (21). Hence, the optimal power can be obtained by using the Lagrangian optimization approach as follows:

$$\begin{aligned} L\left(P(z_s, z_{sp}), \lambda\right) &= \mathbb{E}\left\{\mathcal{I}\left(P(z_s, z_{sp}) z_s\right)\right\} \\ &\quad + \lambda\left(Q_{\text{avg}} - \mathbb{E}\left\{P(z_s, z_{sp}) z_{sp}\right\}\right) \quad (55) \\ &= \mathbb{E}\left\{\mathcal{I}\left(P(z_s, z_{sp}) z_s\right) - \lambda P(z_s, z_{sp}) z_{sp}\right\} \\ &\quad + \lambda Q_{\text{avg}}. \quad (56) \end{aligned}$$

Above, λ denotes the nonnegative Lagrange multiplier. The Lagrange dual problem is defined as

$$\min_{\lambda \geq 0} \max_{0 \leq P(z_s, z_{sp}) \leq P_{\text{pk}}} L\left(P(z_s, z_{sp}), \lambda\right). \quad (57)$$

For a fixed λ and each fading state, the subproblem is expressed, by applying the Lagrange dual decomposition method [34], as

$$\max_{0 \leq P(z_s, z_{sp}) \leq P_{\text{pk}}} \mathcal{I}\left(P(z_s, z_{sp})\, z_s\right) - \lambda P(z_s, z_{sp}) z_{sp}. \quad (58)$$

According to the Karush-Kuhn-Tucker (KKT) conditions, the optimal power control $P^*(z_s, z_{sp})$ must satisfy the following:

$$g\left(P(z_s, z_{sp})\right) = \text{MMSE}\left(P(z_s, z_{sp}) z_s\right) z_s \log_2 \mathrm{e} - \lambda z_{sp} = 0, \quad (59)$$

$$\lambda\left(\mathbb{E}\left\{P(z_s, z_{sp}) z_{sp}\right\} - Q_{\text{avg}}\right) = 0, \quad (60)$$

$$\lambda \geq 0, \quad (61)$$

$$\mathbb{E}\left\{P(z_s, z_{sp}) z_{sp}\right\} - Q_{\text{avg}} \leq 0. \quad (62)$$

In (59), we have used the relation between the mutual information and MMSE given in (6). It is observed from the constraint in (20), and the conditions in (60)–(62) that if $\mathbb{E}\{z_{sp}\} \leq \frac{Q_{\text{avg}}}{P_{\text{pk}}}$, then the average interference power constraint in (21) is loose. Therefore, $\lambda = 0$ and $P^*(z_{sp}, z_s) = P_{\text{pk}}$. If $\mathbb{E}\{z_{sp}\} > \frac{Q_{\text{avg}}}{P_{\text{pk}}}$, then $\lambda > 0$. Hence, by solving (59), the optimal transmit power can be obtained as

$$P^*(z_{sp}, z_s) = \frac{1}{z_s} \text{MMSE}^{-1}\left(\frac{\lambda z_{sp}}{\log_2 \mathrm{e}\, z_s}\right). \quad (63)$$

Incorporating the nonnegativity of the transmit power, noting that $\text{MMSE}^{-1}(1) = 0$, and combining (63) with (20) yield the desired result in (22). □

B. Proof of Theorem 2

It is easy to show that the optimization problem is a concave maximization problem. Hence, following the same approach adopted in the proof of Theorem 1, the original problem reduces to solving a series of subproblems one for each fading state as follows:

$$\max_{0 \leq P(z_s, z_{sp}) \leq \frac{Q_{\text{pk}}}{z_{sp}}} \mathcal{I}\left(P(z_s, z_{sp}) z_s\right) - \mu P(z_s, z_{sp}). \quad (64)$$

Applying the KKT conditions leads to the following set of equations and inequalities:

$$h\left(P(z_s, z_{sp})\right) = \text{MMSE}\left(P(z_s, z_{sp}) z_s\right) z_s \log_2 \mathrm{e} - \mu = 0, \quad (65)$$

$$\mu\left(\mathbb{E}\left\{P(z_s, z_{sp})\right\} - P_{\text{avg}}\right) = 0, \quad (66)$$

$$\mu \geq 0, \quad (67)$$

$$\mathbb{E}\left\{P(z_s, z_{sp})\right\} - P_{\text{avg}} \leq 0 \quad (68)$$

It is observed from the constraint in (26), and the conditions in (66)–(68) that if $\mathbb{E}\{\frac{Q_{\text{pk}}}{z_{sp}}\} \leq P_{\text{pk}}$, then the average power constraint in (25) is loose. Therefore, $\mu = 0$ and $P^*(z_{sp}, z_s) = \frac{Q_{\text{pk}}}{z_{sp}}$. If $\mathbb{E}\{\frac{Q_{\text{pk}}}{z_{sp}}\} > P_{\text{pk}}$, then $\mu > 0$. Hence, the optimal transmit power can be obtained as follows by solving (65):

$$P^*(z_{sp}, z_s) = \frac{1}{z_s} \text{MMSE}^{-1}\left(\frac{\mu}{\log_2 \mathrm{e}\, z_s}\right). \quad (69)$$

Hence, we can obtain the closed-form optimal power policy in (27) by combining (69), (26) and the nonnegativity of the transmit power. □

C. Proof of Theorem 3

The Lagrangian is expressed as

$$\begin{aligned} &L\left(P(z_s,z_{sp}),\lambda,\mu\right) \\ &\quad=\mathbb{E}\left\{\mathcal{I}\left(P(z_s,z_{sp})z_s\right)\right\}-\mu\left(\mathbb{E}\left\{P(z_s,z_{sp})\right\}-P_{\text{avg}}\right) \\ &\quad\quad-\lambda\left(\mathbb{E}\{P(z_s,z_{sp})z_{sp}\}-Q_{\text{avg}}\right). \end{aligned} \tag{70}$$

Applying the KKT conditions results in the following equation, we have

$$\eta\left(P(z_s,z_{sp})\right)=\text{MMSE}\left(P(z_s,z_{sp})z_s\right)z_s\log_2\mathrm{e}-\mu-\lambda z_{sp}=0. \tag{71}$$

Solving the above equation gives the desired result in (31).

D. Proof of Theorem 4

In the low power regime, MMSE behaves as [22]

$$\text{MMSE}(\rho)=\dot{\mathcal{I}}(0)+\ddot{\mathcal{I}}(0)\rho+o(\rho^2) \tag{72}$$

where $\dot{\mathcal{I}}(0)=1$ [22]. Incorporating the above second-order approximation into (59), we obtain

$$\left(1+\ddot{\mathcal{I}}(0)P(z_s,z_{sp})z_s\right)z_s\log_2\mathrm{e}-\lambda z_{sp}=0. \tag{73}$$

Solving the above equation, and then combining the corresponding result with the peak transmit power constraint in (20) and the nonnegativity of the transmission power provides the optimal power policy in (42). □

REFERENCES

[1] P. Steenkiste, D. Sicker, G. Minden, and D. Raychaudhuri, "Future directions in cognitive radio network research," presented at the NSF Workshop, Arlington, VA, USA, 2009.

[2] "Spectrum policy task force," Fed. Commun. Comm., Washington, DC, USA, Rep. ET Docket 02-135, Nov. 2002.

[3] J. Mitola and G. Q. Maguire, "Cognitive radio: Making software radios more personal," *IEEE Pers. Commun.*, vol. 6, no. 6, pp. 13–18, Aug. 1999.

[4] C. Stevenson *et al.*, "IEEE 802.22: the first cognitive radio wireless regional area network standard," *IEEE Commun. Mag.*, vol. 47, no. 1, pp. 130–138, Jan. 2009.

[5] A. Flores, R. Guerra, E. Knightly, P. Ecclesine, and S. Pandey, "IEEE 802.11af: A standard for TV white space spectrum sharing," *IEEE Commun. Mag.*, vol. 51, no. 10, pp. 92–100, Oct. 2013.

[6] F. Granelli *et al.*, "Standardization and research in cognitive and dynamic spectrum access networks: IEEE SCC41 efforts and other activities," *IEEE Commun. Mag.*, vol. 48, no. 1, pp. 71–79, Jan. 2010.

[7] "Second report and order and memorandum opinion and order," Fed. Commun. Comm., Washington, DC, USA, ET Docket 08-260, Nov. 2008.

[8] E. Biglieri, A. J. Goldsmith, L. J. Greenstein, N. B. Mandayam, and H. V. Poor, *Principles of Cognitive Radio*. Cambridge, U.K.: Cambridge Univ. Press, 2013.

[9] E. Hossain, D. Niyato, and Z. Han, *Dynamic Spectrum Access and Management in Cognitive Radio Networks*. Cambridge, U.K.: Cambridge Univ. Press, 2009.

[10] A. Goldsmith, S. A. Jafar, I. Maric, and S. Srinivasa, "Breaking spectrum gridlock with cognitive radios: An information theoretic perspective," *Proc. IEEE*, vol. 97, no. 5, pp. 894–914, May 2009.

[11] L. Musavian and S. Aissa, "Outage-constrained capacity of spectrum-sharing channels in fading environments," *IET Commun.*, vol. 2, no. 6, pp. 724–732, Jul. 2008.

[12] X. Kang, R. Zhang, Y.-C. Liang, and H. K. Garg, "Optimal power allocation strategies for fading cognitive radio channels with primary user outage constraint," *IIEEE J. Sel. Areas Commun.*, vol. 29, no. 2, pp. 374–383, Feb. 2011.

[13] X. Kang, R. Zhang, Y.-C. Liang, and H. K. Garg, "Optimal power allocation for cognitive radio under primary user outage capacity constraint," in *Proc. IEEE ICC*, Jun. 2009, pp. 1–5.

[14] X. Kang, H. K. Garg, Y.-C. Liang, and R. Zhang, "Optimal power allocation for OFDM-based cognitive radio with new primary transmission protection criteria," *IEEE Trans. Wireless Commun.*, vol. 9, no. 6, pp. 2066–2075, Jun. 2010.

[15] L. Musavian and S. Aissa, "Capacity and power allocation for spectrum-sharing communications in fading channels," *IEEE Trans. Wireless Commun.*, vol. 8, no. 1, pp. 148–156, Jan. 2009.

[16] X. Kang, Y.-C. Liang, A. Nallanathan, H. K. Garg, and R. Zhang, "Optimal power allocation for fading channels in cognitive radio networks: Ergodic capacity and outage capacity," *IEEE Trans. Wireless Commun.*, vol. 8, no. 2, pp. 940–950, Feb. 2009.

[17] L. Musavian and S. Aissa, "Effective capacity of delay-constrained cognitive radio in Nakagami fading channels," *IEEE Trans. Wireless Commun.*, vol. 9, no. 3, pp. 1054–1062, Mar. 2010.

[18] M. Jung, K. Hwang, and S. Choi, "Joint mode selection and power allocation scheme for power-efficient Device-to-Device (D2D) communication," in *Proc. IEEE VTC Spring*, May 2012, pp. 1–5.

[19] M. Belleschi, G. Fodor, and A. Abrardo, "Performance analysis of a distributed resource allocation scheme for D2D communications," in *Proc. IEEE GLOBECOM Workshops*, Dec. 2011, pp. 358–362.

[20] P. Cheng, L. Deng, H. Yu, Y. Xu, and H. Wang, "Resource allocation for cognitive networks with D2D communication: An evolutionary approach," in *Proc. IEEE WCNC*, Apr. 2012, pp. 2671–2676.

[21] M. C. Erturk, S. Mukherjee, H. Ishii, and H. Arslan, "Distributions of transmit power and SINR in device-to-device networks," *IEEE Commun. Lett.*, vol. 17, no. 2, pp. 273–276, Feb. 2013.

[22] A. Lozano, A. M. Tulino and S. Verdú, "Optimum power allocation for parallel Gaussian channels with arbitrary input distributions," *IEEE Trans. Inf. Theory*, vol. 52, no. 7, pp. 3033–3051, Jul. 2006.

[23] D. Guo, S. Shamai, and S. Verdú, "Mutual information and minimum mean-square error in Gaussian channels," *IEEE Trans. Inf. Theory*, vol. 51, no. 4, pp. 1261–1283, Apr. 2005.

[24] K. D. Nguyen, A. Guillen i Fabregas, and L. K. Rasmussen, "Power allocation for block-fading channels with arbitrary input constellations," *IEEE Trans. Wireless Commun.*, vol. 8, no. 5, pp. 2514–2523, May 2009.

[25] L. Sboui, Z. Rezki, and M.-S. Alouini, "Capacity of spectrum sharing cognitive radio systems over nakagami fading channels at low SNR," in *Proc. IEEE ICC*, Jun. 2013, pp. 5674–5678.

[26] A. Goldsmith, *Wireless Communications*. Cambridge, U.K.: Cambridge Univ. Press, 2005.

[27] M.-S. Alouini and A. J. Goldsmith, "Capacity of Rayleigh fading channels under different adaptive transmission and diversity-combining techniques," *IEEE Trans. Veh. Technol.*, vol. 48, no. 4, pp. 1165–1181, Jul. 1999.

[28] J. M. Peha, "Approaches to spectrum sharing," *IEEE Commun. Mag.*, vol. 43, no. 2, pp. 10–12, Feb. 2005.

[29] Q. Zhao, S. Geirhofer, L. Tong, and B. M. Sadler, "Opportunistic spectrum access via periodic channel sensing," *IEEE Trans. Signal Process.*, vol. 56, no. 2, pp. 785–796, Feb. 2008.

[30] M. Abramovitz and I. A. Stegun, *Handbook of Mathematical Functions*, Applied Mathematics Series. Gaithersburg, MD, USA: National Bureau of Standards, 1965.

[31] S. Boyd, L. Xiao, and A. Mutapcic, "Subgradient methods," in *Lecture Notes of EE392o*. Standford, CA, USA: Standford Univ. Press, Autumn Quart. 2003/2004.

[32] M. Abramowitz and I. A. Stegun, *Handbook of Mathematical Functions with Formulas, Graphs, and Mathematical Tables*. 9th ed. New York, NY, USA: Dover, 1970.

[33] K. Aomoto and M. Kita, *Theory of Hypergeometric Functions*. Berlin, Germany: Springer-Verlag, 2011.

[34] D. Palomar and M. Chiang, "A tutorial on decomposition methods for network utility maximization," *IEEE J. Sel. Areas Commun.*, vol. 24, no. 8, pp. 1439–1451, Aug. 2006.

[35] I. S. Gradshteyn and I. M. Ryzhik, *Table of Integrals, Series, and Products*, 7th ed. San Diego, CA, USA: Academic, 2007.

[36] R. M. Corless, G. H. Gonnet, D. E. G. Hare, D. J. Jeffrey, and D. E. Knuth, "On the Lambert W function," *Adv. Comput. Math.*, vol. 5, no. 1, pp. 329–359, 1996.

[37] Z. Rezki and M.-S. Alouini, "On the capacity of Nakagami-m fading channels with full channel state information at low SNR," *IEEE Wireless Commun. Lett.*, vol. 1, no. 3, pp. 253–256, Jun. 2012.

Gozde Ozcan received the B.S. degree in electrical and electronics engineering from Bilkent University, Ankara, Turkey in 2011. She is currently working towards the Ph.D. degree in the Department of Electrical Engineering and Computer Science, Syracuse University, Syracuse, NY USA. She has been TPC member of VTC2014-Fall. Her research interests are in the fields of wireless communications, radio resource management, energy-efficient transmission techniques, statistical signal processing, and cognitive radio systems.

M. Cenk Gursoy received the B.S. degree (with high distinction) in electrical and electronics engineering from Bogazici University, Istanbul, Turkey, in 1999 and the Ph.D. degree in electrical engineering from Princeton University, Princeton, NJ, USA in 2004. He was a recipient of the Gordon Wu Graduate Fellowship from Princeton University between 1999 and 2003. In the summer of 2000, he worked at Lucent Technologies, Holmdel, NJ, USA, where he conducted performance analysis of DSL modems. Between 2004 and 2011, he was a faculty member in the Department of Electrical Engineering at the University of Nebraska-Lincoln (UNL), Lincoln, NE, USA. He is currently an Associate Professor in the Department of Electrical Engineering and Computer Science at Syracuse University, Syracuse, NY, USA. His research interests are in the general areas of wireless communications, information theory, communication networks, and signal processing. He is currently a member of the editorial boards of IEEE TRANSACTIONS ON WIRELESS COMMUNICATIONS, IEEE TRANSACTIONS ON COMMUNICATIONS, IEEE TRANSACTIONS ON VEHICULAR TECHNOLOGY, and *Physical Communication (Elsevier)*. He served as an editor for IEEE COMMUNICATIONS LETTERS between 2012 and 2014. He received an NSF CAREER Award in 2006. More recently, he received the EURASIP Journal of Wireless Communications and Networking Best Paper Award, the UNL College Distinguished Teaching Award, and the Maude Hammond Fling Faculty Research Fellowship.